The Unexpected Role of Arsenic in Driving the Selective Growth of InAs Quantum Dots on GaAs

Fabrizio Arciprete,[†,*] Ernesto Placidi,[†,‡] Rita Magri,[§] Massimo Fanfoni,[†] Adalberto Balzarotti,[†] and Fulvia Patella[†]

[†]Dipartimento di Fisica, Università di Roma "Tor Vergata", Via della Ricerca Scientifica 1, I-00133 Roma, Italy, [‡]CNR-ISM, Via Fosso del Cavaliere 100, I-00133 Roma, Italy, and [§]Dipartimento di Fisica, Università di Modena e Reggio Emilia, and Centro S3 CNR-Istituto Nanoscienze, Via Campi 213/A, 4100 Modena, Italy

ABSTRACT Here we show a new effect due to the arsenic flux in the molecular beam epitaxy growth of InAs quantum dots on GaAs(001) at temperatures higher than 500 °C and high As/In flux ratio. We show that, by changing and tuning the direction of the As flux on a rippled substrate, a selective growth can be obtained where the dots form only on some appropriately orientated slopes of a sequence of mounds elongated along the [$\bar{1}$10] surface direction. Since the relative As flux intensity difference over the two opposite mound slopes is very small (2−5%), the observed large effect cannot be explained simply as a pure shadowing effect and reveals instead that As, whose contribution to the modeling of growth has often been ignored or underestimated, probably for a lack of knowledge, plays a fundamental role at these growth conditions. To explain our experiment, we have developed a kinetic model that explicitly takes into account the coupling between cations (In) and anions (As) and found that the very small surface gradient in the anion flux, due to the oblique evaporation on the mounded surface, is responsible for a massive drain of cations toward the surface anion-rich areas, thus generating the selective growth of quantum dots. We expect a comparable behavior for the anions of other III−V and II−VI compound semiconductors.

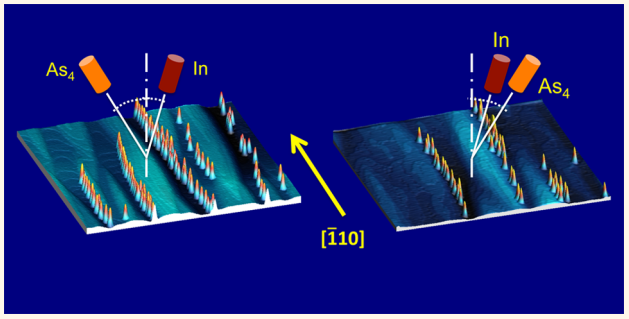

KEYWORDS: quantum dots · molecular beam epitaxy · kinetic modeling · rate equations

The attractive prospects of quantum dots (QDs) have been demonstrated in the case of sophisticated applications in new-generation devices such as single-photon emitters for nanophotonics and quantum computing.[1−3] In the past decade, a considerable amount of research has been devoted to the attempt to employ the Stranski−Krastanov growth mode in highly strained semiconductor heteroepitaxy in order to engineer defect-free, spatially ordered, self-assembled QDs. Until now, advances in this regard have been obtained by combining bottom-up and top-down methods, such as introducing *ex situ* processing steps (*e.g.*, standard lithography) before and/or after the epitaxial growth[4−6] or by multilayer stacking.[7−9]

It is well known that steps and step bunching constitute preferential sites for dot nucleation.[10−14] In this paper we report on a new effect due to the As flux direction that can take place on structured substrates when InAs is deposited at high growth temperature and at high V/III flux ratios. We show that at these growth conditions by tuning the As flux direction it is possible to decide which slopes, among all the otherwise similar step-bunching slopes, will accommodate the growing dots, adding in this way a further degree of freedom for nonrandomness in the system. We find indeed that the dots grow only on the step bunching of the pattern oriented toward the incoming As flux.

This selective growth can be obtained in principle by (i) engineering a proper step-bunching arrangement on the buffer layer and (ii) appropriately tuning the directions of the As flux at growth temperatures higher than 500 °C. In order to demonstrate the effect, we create a step bunching by intentionally inducing (by a suitable choice of the growth parameters[15,16]) the formation of surface instabilities during the growth of the buffer layer, so as to obtain a slightly

* Address correspondence to fabrizio.arciprete@roma2.infn.it.

Received for review October 12, 2012 and accepted April 8, 2013.

Published online April 08, 2013
10.1021/nn401338v

rippled surface consisting of a sequence of mounds elongated along the [$\bar{1}$10] surface direction. The oblique incidence of the As flux on the surface during the InAs deposition at a growth temperature of 545 °C leads then to the formation of QDs aligned along *only one* of the two sides of the mounds, *i.e.*, the one facing the As flux. The opposite side along with the flat regions of the substrate surface are completely bare of dots. Given the small tilting angles of the mound sides, shadowing effects cannot explain our observation.

These findings contradict the minor role usually attributed to anions in the III−V molecular beam epitaxy (MBE) growth. Growth is indeed commonly described as primarily dictated by the dynamics of cations, assumed as the rate-limiting species. Our experiment shows instead that, at the growth conditions used, As has a strong influence on the nucleation and development of the InAs islands, and its contribution cannot be neglected in the description of the growth process.

To explain the experiment, we have developed a kinetic model that introduces couplings between In and As atoms. We have found that the small As flux gradient existing between the two mound sides, because of the oblique As evaporation, acts as a pump, pushing the cations from one side to the other side of the mounds. This causes the growth of the dots on only one of the two mound sides. This In surface current is generated by the inhomogeneity in the In adatom surface distribution caused by the As flux intensity gradient and is activated by the relatively high growth temperatures. Here, we find that the As-related In adatom density gradient between the two mound sides is not only due to reasons of equilibrium between the As on the surface and the As vapor pressure;[17] it is also a distinct byproduct of the incorporation dynamics, where As plays an important role. Our kinetic model of dot growth incorporates many new features such as (i) a different dynamics for cations and anions, (ii) a distinction between the bulk and surface regions of the dot, and (iii) a dot surface composition that depends primarily on the growth conditions (substrate temperature, atomic and molecular fluxes).

EXPERIMENTAL RESULTS

The samples were prepared by molecular beam epitaxy on singular GaAs(001) substrates. It is well known that the growth of GaAs films in the presence of step edge barriers can be unstable on low-index crystal surfaces, which can develop step bunching, forming large mounded structures with a typical slope of a few degrees.[15] As these structures can provide a template for the nucleation sites of QDs, we intentionally induced the formation of surface instabilities during the growth of the buffer layer by means of a suitable choice of the growth parameters[15,16] (see Figure 1). The deposition of 2.45 ML of InAs was performed at 545 °C with a pulsed In flux (pulsed deposition (PD) mode, each pulse being 5 s of evaporation followed by 25 s of growth interruption) and a continuous As_4 flux, without rotating the sample and for different orientations of the As_4 flux with respect to the normal direction to the sample surface (Figure 1). (See Experimental Methods section for more details.)

The anisotropic surface distribution of QDs is shown in Figure 1, where the atomic force microscopy (AFM) topographies of three different samples are reported together with the schematic drawings of the evaporation geometry used for each sample. In particular, the figure shows the orientation of the As_4 and In fluxes with respect to the plane (110) of the samples. The images show the rippled morphology of the substrates, made of mounds elongated along the [$\bar{1}$10] direction, produced by the kinetic instabilities during the buffer layer growth. Very importantly, the topographies of Figure 1 also show the strict correlation between the growth conditions and the resulting surface distribution of QDs. When the InAs is deposited with a pulsed In flux, the sample rotation is switched off; there is also a given orientation of the As_4 flux with respect to the plane (110) of the sample (see the drawings in Figure 1); as a result, the QDs are aligned along the step bunching of one single side of the mounds (Figure 1b,c). Such asymmetry is strongly reduced when the growth is performed with the same growth rate but with a continuous In flux (continuous deposition (CD) mode)) (Figure 1a) and vanishes completely when the sample rotation is switched on (Figure S1 in the Supporting Information). In Table 1 all the relevant parameters determined by a statistical analysis of many AFM topographies for each sample are reported with respect to the growth conditions.

It is clearly evident that the mound side where the QDs are located is determined by the direction from where the As_4 beam comes from. In fact, if we reverse the direction of the As_4 beam (Figure 1b,c), the mound side where the QDs are located is reversed as well. The percentage of asymmetry in the QDs position-related density, $f_{\rho_{left}}(\%) = (\rho_{left}/\rho_{left})100$, where ρ is the QDs number density, increases as a function of the angle between the As_4 beam direction and the plane (110). As can be seen in Figure 1b,c and Table 1, the surface distribution of QDs is completely asymmetric when the angle of incidence of the As_4 beam is $\theta_{As_4} = 25°$ and $\theta_{As_4} = -27°$ with $f_{\rho_{left}} = 99\%$ and $f_{\rho_{left}} = 5\%$, respectively. A significant (32%) QD formation on the side of the mounds opposite the As flux is observable only when the angle of incidence of the As_4 beam is decreased to 16° (Figure S1 in the Supporting Information) or when the sample is grown with the CD mode ($f_{\rho_{left}} = 59\%$, Figure 1a).

Figure 2b shows an AFM image of a sample grown by PD mode but with a lower InAs deposition (2.1 ML). The sample was quenched at the end of the growth cycle subsequent to the cycle for which the critical

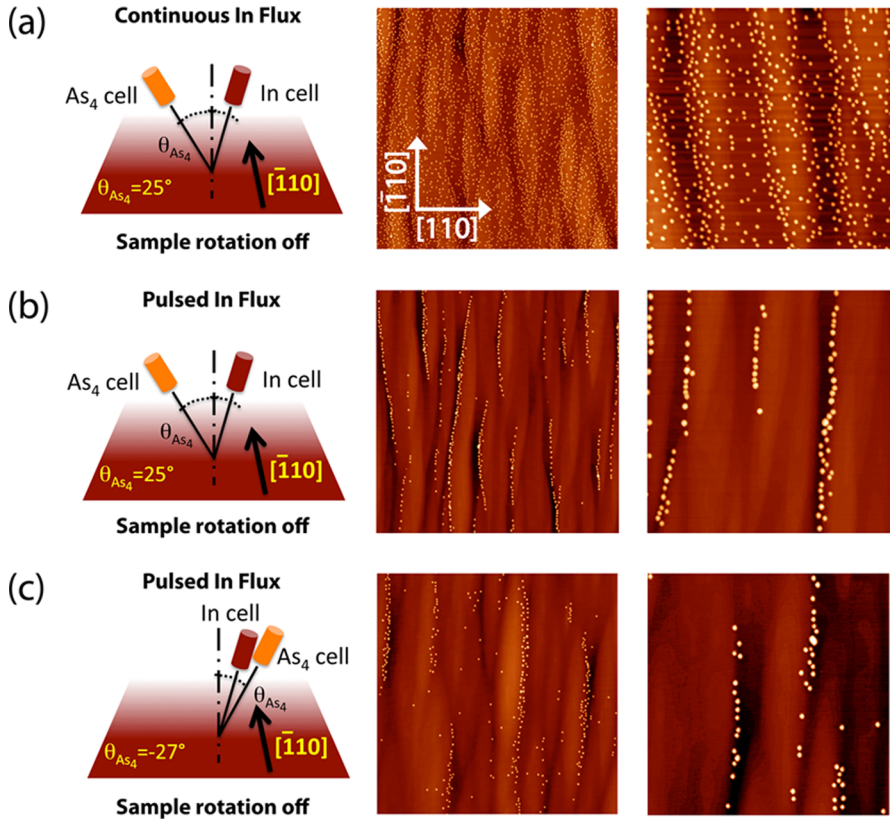

Figure 1. Schematic drawings of evaporation (left column) and AFM topographies, 5 × 5 μm^2 (center column) and 2 × 2 μm^2 (right column), revealing the decoration of the step bunching on one side of the mounds (b, c) after deposition of 2.45 ML of InAs at T = 545 °C. The depositions were carried out without rotating the sample, with different growth procedures (continuous and pulsed In flux, with a continuous As_4 flux), and with different orientations of the As_4 beam with respect to the plane (110) of the sample. (a) Continuous In flux; $\theta_{As_4} = 25°$. (b) Pulsed In flux; $\theta_{As_4} = 25°$. (c) Pulsed In flux; $\theta_{As_4} = -27°$.

TABLE 1. Number Density (ρ) of QDs and Percentage of Asymmetry ($f_{\rho left}$(%) = (ρ_{left}/ρ)100), Determined by a Statistical Analysis of Many AFM Topographies, with Respect to the Growth Mode (GM), Geometry of Evaporation, and Temperature of Growth (T_{growth})

GM	SR[a]	T_{growth} (°C)	As_4 cell angle (deg)	ρ (cm^{-2})	$f_{\rho left}$ (%)
PD[b]	off	500	25° left	2.9×10^{10}	64
PD	off	530	25° left	4.0×10^{9}	97
PD	on	545	25° left	1.1×10^{9}	50
PD	off	545	25° left	1.7×10^{9}	99
PD	off	545	16° left	2.9×10^{9}	68
PD	off	545	27° right	1.1×10^{9}	5
CD[c]	off	545	25° left	1.1×10^{10}	59
PD[d]	off	545	25° left	1.3×10^{9}	74

[a] SR, sample rotation. [b] PD, pulsed In flux. [c] CD, continuous In flux. [d] InAs coverage 2.1 ML.

thickness was reached. The image shows that, at the critical thickness for the 2D to 3D transition, QDs are nucleated on both sides of the mounds, although, at the stage of the growth reported in the figure, the dots on the right side already have a significantly smaller density ($f_{\rho_{left}}$ = 74%; see Table 1) and size.

The observed phenomenology clearly demonstrates that the orientation of the As_4 beam plays a crucial role in the selective growth of QDs. Conversely, the orientation of the In flux is not significant, being always the same for all the samples grown and almost vertical with respect to the sample surface (θ_{In} = 12° on the right side with reference to the drawings in Figure 1). The mounds on the substrate surface are fully symmetric (the average slope along the [110] direction is in the range 1−3°, from sample to sample): Thus any possible effect related to different slopes between the two sides of the mounds can be ruled out. Furthermore, the low average slope of the mound sides allows us to exclude shadowing effects for both As and In fluxes (see Figure 2a, where the mounds are schematized and represented in scale). Shadowing effects, related to In flux, have recently been reported in the case of mounds with very steep facets.[18] Actually, the evaporation geometry (Figure 2a) allows for a tiny difference between the As_4 fluxes on the opposite sides of the mounds. By considering an As_4 incidence angle θ_{As_4} = 25−27° and the average slope of the mound sides, the relative difference between the effective projected flux on the two mound sides is, on average, $\Delta F_{As_4}/F_{As_4} \approx 1-5\%$.

Other than the As_4 flux direction, another key parameter for obtaining the selective growth of QDs is the

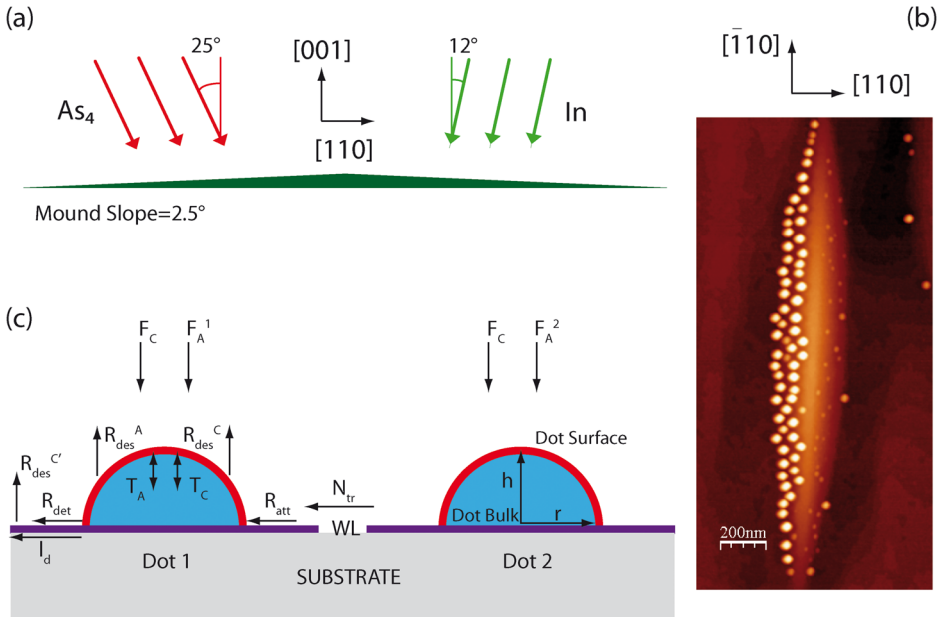

Figure 2. (a) Schematic side view of a typical mound represented in scale; the lateral slope is 2.5°. The orientations of the As_4 and In beams with respect to the sample normal are also reported. (b) AFM topography $1 \times 2\ \mu m^2$ after deposition of 2.1 ML of InAs at $T = 545$ °C. The image shows that, immediately after the 2D to 3D growth-mode transition, nucleation of QDs occurs on both sides of a mound. (c) Schematic side view of two dots of radius r and height h with their bulk and surface, sitting on top of the surrounding wetting layer (WL) on the two sides of a mound. On the left, the directions of the atomic exchanges, coupling the different subsystems (dot−bulk, dot−surface, WL, and vapor phase), are indicated by arrows, and their expressions are given in the text. The arrow labeled with N_{tr} represents the coupling between the two dots.

substrate temperature: it must be greater than ~530 °C (although, to a much lesser extent, the effect is still present at lower temperatures starting from about 500 °C; see Table 1). It is well known[19,20] that, above 500 °C, InAs dots are formed only if the As/In flux ratio is greater than a given value, and the higher the temperature, the greater the need for the As flux intensity. Above 550 °C, no InAs islands are formed irrespective of the As flux.[19,21] This behavior has been ascribed to temperature-activated indium desorption.[20,21] It is clear, however, that at the growth temperature employed in the present work (545 °C) we are close to these critical conditions; hence In desorption cannot be neglected.

THEORETICAL RESULTS

To explain the experiment, we have developed a kinetic model that predicts the time evolution of 3D islands from the appearance of small structures (radius 1−2 nm) and throughout cycles of 5 s of growth and subsequent 25 s of annealing period (PD growth mode). We first note that at T = 545 °C nuclei can stabilize preferably at the step bunching, where, due to a higher density of dangling bonds, the adatoms find more stable binding sites.[10−14] Thus, we assume that stable nuclei occur only at the mound sides. We study the time evolution of two dots assumed to be nucleated on the two sides of a mound. This assumption is substantiated by the AFM topography shown in Figure 2b. Then we model the dots as positioned on two planar surfaces subjected to slightly different As molecular fluxes (F_A^1 and F_A^2 in Figure 2c). Indeed, the local surface density of As tetramers is the only experimentally relevant difference existing between the two sides of the mounds.

Each dot is coupled to the external fluxes and to a portion of the surrounding wetting layer (WL) (Figure 2c). We first consider the dot−WL system open to atom exchanges with the vapor, but closed to atom exchanges *via* WL with the other dots. Indium atoms (indicated as cations C), after deposition, diffuse randomly inside each dot−WL region and attach to/detach from the dot. The As dimers follow instead a different kinetics. Each As_4 molecule from the flux gives rise to only one As_2 molecule, which may be incorporated at the surface.[22] As_2 molecules are known to be weakly trapped in a precursor state, where they are assumed to be distributed all over the system.[22−24] The As_2 sticking coefficient was found to depend on the availability of cations on the surface.[25] The WL is modeled *via* an ensemble of rapidly diffusing cations. Indeed, experimental observations[26,27] have found that, for In depositions larger than about 1 ML up to the critical thickness, cations become unable to stick to the surface because of the mismatch-related strain and diffuse rapidly on the WL.

The model is expressed through a set of coupled rate equations describing the time evolution of the number of atoms of each species: anions and cations at the dot surface, anions and cations in the dot bulk, and fast diffusing cations on the WL surface. The WL is modeled

as a circular sector surrounding the dot, whose width depends on the cation diffusing length $l_d = a_o(R_{diff}t_d)^{1/2}$, where R_{diff} is the cation diffusion rate, a_o the lattice parameter, and t_d the WL cation diffusion lifetime, for which we assume the value of 1 s, consistent with a relatively long diffusion length at the high growth temperatures. Thus, the diffusion length comes to depend on the temperature, but not explicitly on the As flux because of our simplified model of the WL. We label $N_C^s(t)$ and $N_A^s(t)$ the number of In and As atoms at the dot surface at time t, and $N_C^{WL}(t)$ the number of In atoms diffusing randomly on the WL surface.[26−28] Their time evolution is given by

$$\frac{dN_C^s}{dt} = F_C S_{dot} - R_{des}^C N_C^s + \frac{1}{4}R_{att}N_C^{WL} - R_{det}f_{N_C^s} - T_C^{s\to b} + T_C^{b\to s} \quad (1)$$

$$\frac{dN_A^s}{dt} = F_A'\frac{\lambda}{d_C}S_{dot} - R_{des}^A N_A^s - T_A^{s\to b} + T_A^{b\to s} \quad (2)$$

$$\frac{dN_C^{WL}}{dt} = F_C S_{WL} - R_{des}^{C'} N_C^{WL} - \frac{1}{4}R_{att}N_C^{WL} + R_{det}f_{N_C^s} \quad (3)$$

F_C is the incident flux of In atoms. In the case of As, by assuming that the incorporation occurs only when the As dimer is in the precursor state and encounters an appropriate cation site,[22−24] we obtain an incorporation rate that depends explicitly on the number of surface In atoms as $F_A'(\lambda/d_C)$, where $F_A' = F_A \exp(E_B/kT)$ is the enhancement of the incident flux F_A due to the entrapment of the As_2 molecules in the precursor with barrier E_B = 0.25 eV (see Supporting Information). $\lambda = \tau(2\pi kT/m)^{1/2}$ is the distance traveled by the As_2 molecule during its lifetime $\tau \approx 10^{-12}$ s, m is the molecule mass, and d_C is the average distance between two surface indium atoms. Other events occurring for both species at the dot surface include desorption (with rates R_{des}) and transfer to and from the dot bulk (T). Only cations are assumed to diffuse and attach to (with rate R_{att}) and detach from (with rate R_{det}) the dot border (see Supporting Information). The number of In atoms on the dot border is given by $f_{N_C^s}$ in terms of the surface atoms N_C^s and of the ratio between surface area and perimeter. For simplicity the dot is assumed to have the shape of a spherical sector with surface S_{dot}.

The dots grow or dissolve through atom transfer from the surface to the bulk below and *vice versa*. Bulk atoms are fully four-coordinated to atoms of the other species and are inert in regard to the growth events. They evolve as

$$\frac{dN_C^b}{dt} = +T_C^{s\to b} - T_C^{b\to s} = f_1(t)\Psi_A \quad (4)$$

$$\frac{dN_A^b}{dt} = +T_A^{s\to b} - T_A^{b\to s} = f_2(t)\Psi_C \quad (5)$$

where $f_1(t)$ and $f_2(t)$ are introduced for each atomic species, respectively, to express how many bulk atoms of a given species are generated in the average for each incorporated surface atom of the other species. $\Psi_C = F_C S_{dot} - R_{des}^C N_C^s + 1/4\, R_{att}N_C^{WL} - R_{det}f_{N_C^s}$ is the net In flux on the dot surface (the difference between atoms incorporated at and leaving from the surface), while $\Psi_A = F_A'\lambda/d_C\, S_{dot} - R_{des}^A N_A^s$ is the same quantity for As atoms (see Supporting Information for more details).

The kinetic coupled eqs 1−5 are solved using the Runge−Kutta method. We find that, irrespective of the used rates, the dot exposed to the larger flux (Dot 1 in Figure 2c) always has a larger volume than that exposed to the smaller flux (Dot 2 in Figure 2c). The different density of As_2 precursors on the two sides of the mounds also affects, as well as dimension, a number of other dot properties. Regardless of the employed energy barrier values, we always find that Dot 2 has a cation-richer surface composition. Dot 1 is under an As flux of 30 atoms/nm^2 s, whereas Dot 2 is under an As flux of 27 atoms/nm^2 s. The In flux is 0.2 atoms/nm^2 s, with a As/In ratio larger than 100 (see Supporting Information).

Furthermore, we always find a slightly larger density of cations ρ_{WL} in the WL of Dot 2. Thus, the entire surface region of Dot 2 is In-richer than the surface of Dot 1. Eventually we find that a relatively small As surface density gradient originates a gradient in the cation surface density. At the high temperature used in our experiment surface cations have a very large mobility; thus, we expect that the density gradient should originate a cation flow from the mound side, where the As flux is smaller, to the other side. In order to verify this hypothesis, we introduce two new ingredients into our model. The first one is a modification of the detachment barrier taking into account size and composition-related effects (see Supporting Information). Thus, we model the total detachment rate as

$$R_{det}' = R_{det}\frac{l_d^2}{S_{dot}}\left\{\Theta(x_C - 1/2)\exp(2x_C - 1)\frac{E_x}{k_B T}\right\} \quad (6)$$

where x_C is the cation content, $\Theta(x)$ is the Heaviside step function. l_d^2/S_{dot} is the ratio between the surface spanned by the diffusing In on the dot surface and the actual dot surface area, and it is related to the frequency with which surface cations reach the dot border. An increase of the detachment rate for smaller dots is produced without the introduction of a new energy barrier. The factor in the curly brackets increases the detachment rate R_{det}' and then decreases the detachment barrier only for In-rich surfaces and proportionally to the In composition. E_x = 0.45 eV is estimated by the *ab initio* calculations.[29,30] The second ingredient is the coupling between the two dots, that is, the cation transfer between the two dot−WL regions. This is calculated using the Fick law. The number of In atoms transferred per second, $N_{tr}(t)$,

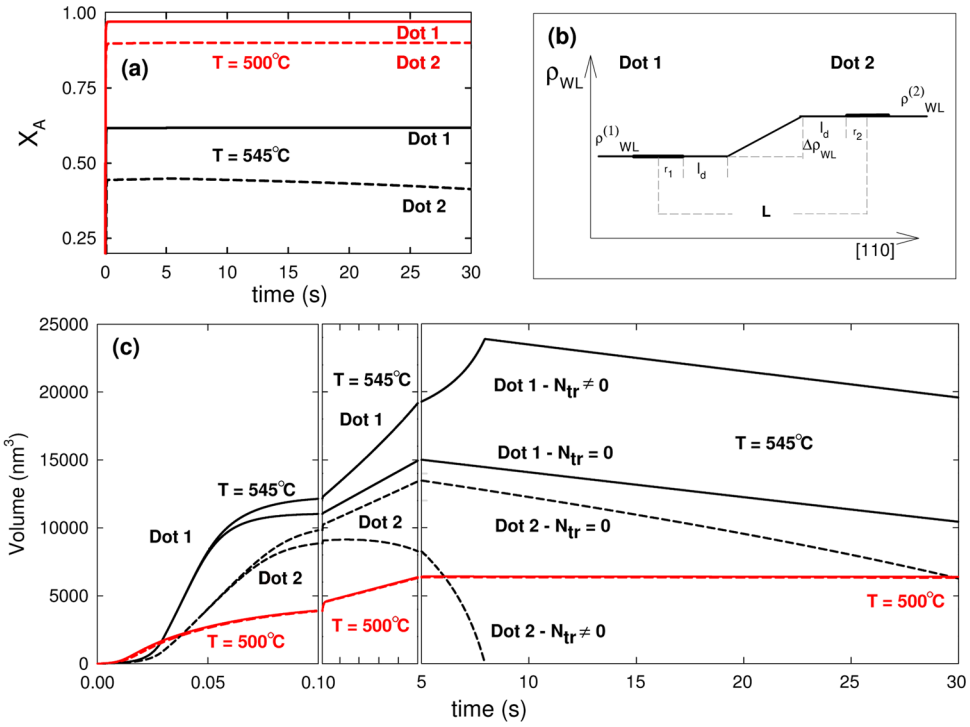

Figure 3. (a) As surface content $x_A = N^s_A/(N^s_A + N^s_C)$ of Dot 1 (solid lines) and Dot 2 (dashed lines) at $T = 500$ °C (red lines) and at $T = 545$ °C (black lines). $x_A = 1$ corresponds to a full As-rich dot surface, and $x_A = 0.5$ to equal As and In content. Dot 1 is under an As flux of 30 atoms/(nm^2 s), whereas Dot 2 is under an As flux of 27 atoms/(nm^2 s); the In flux is 0.2 atoms/(nm^2 s); the As/In flux ratio is larger than 100. (b) Schematics of the density of cation on the WL (ρ_{WL}) *versus* dot distance (see eq 7). (c) Dot 1 (solid lines) and Dot 2 (dashed lines) volume time evolution at $T = 500$ °C (red lines) and at $T = 545$ °C (black lines).

from one WL region to the other is (assuming the two dot regions do not overlap)

$$N_{tr}(t) = -4D\frac{\Delta\rho_{WL}(t)}{L - (r_1(t) + l_d) - (r_2(t) + l_d)}(r_0(t) + l_d) \quad (7)$$

where $r_0(t) = (r_1 + r_2)/2$ is the average base radius of Dot 1 and Dot 2, and L is a typical distance between the dot regions on the two sides of a mound; we use $L = 350$ nm. $D = R_{diff}a_0^2$ is the diffusion constant; $\Delta\rho_{WL}$ is the difference in the cation density between the two WLs (see Figure 3b).

DISCUSSION

The results of the rate equations for a given set of energy barriers (see Supporting Information) are plotted in Figure 3c for the cases with ($N_{tr} \neq 0$) and without ($N_{tr} = 0$) coupling and for two different growth temperatures. As predicted, when the coupling is "on", the cations flow from the region exposed to the smaller As flux to that exposed to the higher As flux. At $T = 545$ °C, the mass transport between the two areas determines the dissolution of Dot 2 within the first 25 s of the annealing cycle, while Dot 1 continues to grow at the expense of Dot 2. Even without this atom transfer, the volume difference between the two dots is fairly large, especially during the annealing period. However, it is worth noting that the dissolution of Dot 2 takes place only when the coupling between the two dots is allowed. This effect is clearly temperature dependent since at $T = 500$ °C no substantial difference in the volume time evolution is found between the two dots, even when the coupling is "on". The processes leading to Dot 2 dissolution are not yet activated for the chosen energy barrier values. This finding is in line with the experimental results where the selective growth is sharp only at the higher temperatures (see Table 1, where $f_{\rho_{left}}$ at $T = 500$ °C is strongly reduced to 68%). Moreover, our experimental observations show that when the angle of the As flux is reduced to 16°, so that $\Delta F_{As_4}/F_{As_4}$ is smaller, the percentage of observed asymmetry is also smaller (Table 1). This behavior is also predicted by the model (not shown) for which the dissolution of Dot 2 is slower when $\Delta F_A/F_A$ is smaller, enabling Dot 2 to survive during the annealing cycles.

Notably, our model sheds light on the main reason for the experimentally observed *selective growth*. First, we notice from Figure 3a that the higher the As flux intensity, the higher the As incorporated at the dot surfaces. At increasing temperatures, As desorption increases, leading to an In enrichment of both the dot surfaces (Figure 3a). For an As desorption barrier lower than 1.70 eV, the Dot 1 surface is still As-rich (anion content $x_A > 0.5$), while the Dot 2 surface is In-rich ($x_A < 0.5$). Consequently, on the basis of eq 6, the In detachment rate from Dot 2 increases, and more In is released into the WL around Dot 2 (the smaller size of Dot 2 may further increase the detachment rate of In

from Dot 2). On the other hand, the In incorporation kinetics is more efficient when more As is available, as testified by the larger volume of Dot 1. Thus, In is incorporated more efficiently into Dot 1 than into Dot 2, thus leaving a larger In density in the WL (ρ_{WL}) surrounding Dot 2 (see Figure 3b). Both processes contribute to increasing the In density around Dot 2 relative to that around Dot 1. This adatom density gradient leads to a persistent In flow from one side of the mound to the other. The overall process promotes the dissolution of the dots on the side opposite the As flux arrival direction.

A very distinct role is played by indium diffusivity. As shown in eq 7 the observed phenomenon requires a relatively high diffusion constant and corresponding diffusion lengths on the order of the distances between the step bunches. We find l_d = 82 nm at T = 500 °C and l_d = 143 nm at T = 545 °C by using a diffusion barrier E_{diff} = 1.34 eV; these values are to be compared with the estimated experimental value of ~240 nm. A typical distance between two mound bunches L is in the range 200−400 nm. Since diffusion depends considerably on temperature, the activation requirements are clearly satisfied only at high growth temperatures. A different choice for the energy barrier values changes not the occurrence of Dot 2 dissolution, but only the time and the annealing cycle, at which dissolution takes place, provided the diffusion length is sufficiently long.

Our model provides a clear interpretation of the experiment, highlighting the main mechanisms responsible for the observed selective growth. We note that the sample grown in CD mode (see Figure 1a and Table 1) shows only a poor selective growth. However, in light of the kinetic processes identified by our model, we expect that a consistent reduction of the growth rate should enhance the selective growth in the CD mode as well.

CONCLUSIONS

The results presented here highlight an unexpected behavior of As in the nucleation and growth of InAs QDs. We have shown that, growing InAs on a slightly rippled GaAs buffer layer with a properly tilted incoming As flux, even a small imbalance in the As flux intensity can lead to a selective growth of QDs at specific locations on the surface. We have developed a kinetic model that shows that such an As gradient can drag In adatoms over the surface, thus determining the positions where the QDs grow, provided the growth temperature is sufficiently high to enhance the In surface mobility. Our results tackle the problem of the comprehension of fundamental aspects of nanostructure growth in III−V systems and, in particular, offer new insights and pose new questions regarding the understanding of the interaction kinetics of anions during the growth of both III−V semiconductors and other compound semiconductors for which the adsorption kinetics of one of the elements involves a highly mobile precursor state close to the surface.

EXPERIMENTAL METHODS

Sample Growth. The samples were prepared by molecular beam epitaxy (RIBER 32P reactor) on singular GaAs(001) substrates with a miscut angle of about 0.01°, corresponding to average step distances of about 2000 nm. A GaAs buffer layer of approximate thickness 500 nm was grown at 590 °C with a choice of the As_4/Ga flux ratio and of the growth rate suitable for inducing the formation of surface instabilities[15,16] (see Figure 1). The InAs depositions were carried out with a pulsed In flux (PD mode) and a continuous As_4 flux, without rotating the sample, for three different orientations of the As_4 flux with respect to the normal direction to the sample surface (Figure 1). The In delivery was cycled in 5 s of evaporation followed by 25 s of growth interruption with the As_4 shutter permanently open. For all the samples studied a deposition of 2.45 ML of InAs was performed at a rate of 0.03 ML/s at 545 °C, a temperature where the stable surface reconstruction of GaAs(001) is (2 × 4). The As_4/In flux ratio was about 40 in order to control the decrease of the In sticking coefficient with temperature.[19,20] Immediately after the InAs growth, the samples were quenched under As_4 flux (beam equivalent pressure = 1.3 × 10^{-6} Torr). For purposes of comparison several samples were prepared under different growth conditions: One sample was grown with the same rates and growth temperatures but with a continuous In flux (CD mode) (Figure 1a). Three other samples were grown by PD with rotation switched on (Figure S1 in the Supporting Information) and by PD with rotation switched off, but at different growth temperatures, 500 and 530 °C, respectively (not shown), or smaller InAs coverage (2.1 ML; see Figure 2b). The results are summarized in Table 1.

Sample Characterization. The reflection high-energy electron diffraction pattern was monitored by a charge-coupled device camera during growth. atomic force microscopy. VEECO multiprobe characterization was performed *ex situ* in the tapping mode by using ultrasharp nonconductive Si tips with a nominal radius of about 2 nm.

Conflict of Interest: The authors declare no competing financial interest.

Supporting Information Available: Details of the rate equation model. Additional AFM images and data in Figure S1. This material is available free of charge *via* the Internet at http://pubs.acs.org.

Acknowledgment. The authors are particularly grateful to A. Rastelli for showing us his unpublished data and for useful scientific discussions, to M. K. Yakes for communications about the paper in ref 18, and to D. Del Gaudio, who performed some of the AFM measurements.

REFERENCES AND NOTES

1. Dousse, A.; Suffczynski, J.; Beveratos, A.; Krebs, O.; Lemaître, A.; Sagnes, I.; Bloch, J.; Voisin, P.; Senellart, P. Ultrabright Source of Entangled Photon Pairs. *Nature* **2010**, *466*, 217–220.
2. Petroff, P. M. Semiconductor Self-Assembled Quantum Dots: Present Status and Future Trends. *Adv. Mater.* **2011**, *23*, 2372–2376.
3. Trotta, R.; Zallo, E.; Ortix, C.; Atkinson, P.; Plumhof, J. D.; Van den Brink, J.; Rastelli, A.; Schmidt, O. G. Universal Recovery of the Energy-Level Degeneracy of Bright Excitons in InGaAs Quantum Dots Without a Structure Symmetry. *Phys. Rev. Lett.* **2012**, *109*, 147401.

4. Kiravittaya, S.; Rastelli, A.; Schmidt, O. G. Advanced Quantum Dot Configurations. *Rep. Prog. Phys.* **2009**, *72*, 046502.
5. Yang, B.; Liu, F.; Lagally, M. G. Local Strain-Mediated Chemical Potential Control of Quantum Dot Self-Organization in Heteroepitaxy. *Phys. Rev. Lett.* **2004**, *92*, 025502.
6. Patella, F.; Arciprete, F.; Placidi, E.; Fanfoni, M.; Balzarotti, A.; Vinattieri, A.; Cavigli, L.; Abbarchi, M.; Gurioli, M.; Lunghi, L.; *et al*. Single Quantum Dot Emission by Nanoscale Selective Growth of InAs on GaAs: A Bottom-Up Approach. *Appl. Phys. Lett.* **2008**, *93*, 231904.
7. Tersoff, J.; Teichert, C.; Lagally, M. G. Self-Organization in Growth of Quantum Dot Superlattices. *Phys. Rev. Lett.* **1996**, *76*, 1675–1678.
8. Wang, Z. M.; Holmes, K.; Mazur, Y. I.; Salamo, G. J. Fabrication of (In,Ga)As Quantum-Dot Chains on GaAs(100). *Appl. Phys. Lett.* **2004**, *84*, 1931–1933.
9. Heidemeyer, H.; Denker, U.; Müller, C.; Schmidt, O. G. Morphology Response to Strain Field Interferences in Stacks of Highly Ordered Quantum Dot Arrays. *Phys. Rev. Lett.* **2003**, *91*, 196103.
10. Leon, R.; Senden, T. J.; Kim, Y.; Jagadish, C.; Clark, A. Nucleation Transitions for InGaAs Islands on Vicinal (100) GaAs. *Phys. Rev. Lett.* **1997**, *78*, 4942–4945.
11. Teichert, C. Self-Organization of Nanostructures in Semiconductor Heteroepitaxy. *Phys. Rep.* **2002**, *365*, 335–432.
12. Aqua, J. N.; Berbezier, I.; Favre, L.; Frisch, T.; Ronda, A. Growth and Self-Organization of SiGe Nanostructures. *Phys. Rep.* **2012**, *522*, 59–189.
13. Placidi, E.; Arciprete, F.; Fanfoni, M.; Patella, F.; Orsini, E.; Balzarotti, A. InAs/GaAs(001) Epitaxy: Kinetic Effects in the Two-Dimensional to Three-Dimensional Transition. *J. Phys.: Condens. Matter* **2007**, *19*, 225006.
14. Hanke, M.; Wang, Z. M.; Mazur, Y. I.; Lee, J. H.; Salamo, G. J.; Schmidbauer, M. Step Bunch Assisted Two Dimensional Ordering of $In_{0.19}Ga_{0.81}As/GaAs$ Quantum Dots on Vicinal GaAs(001) Surfaces. *Appl. Phys. Lett.* **2004**, *84*, 1931–1933.
15. Johnson, M. D.; Orme, C.; Hunt, A. W.; Graff, D.; Sudijono, J.; Sander, L. M.; Orr, B. G. Stable and Unstable Growth in Molecular Beam Epitaxy. *Phys. Rev. Lett.* **1994**, *72*, 116–119.
16. Patella, F.; Arciprete, F.; Placidi, E.; Nufris, S.; Fanfoni, M.; Sgarlata, A.; Schiumarini, D.; Balzarotti, A. Morphological Instabilities of the InAs/GaAs(001) Interface and Their Effect on the Self-Assembling of InAs Quantum-Dot Arrays. *Appl. Phys. Lett.* **2002**, *81*, 2270–2272.
17. Tersoff, J.; Johnson, M. D.; Orr, B. G. Adatom Densities on GaAs: Evidence for Near-Equilibrium Growth. *Phys. Rev. Lett.* **1997**, *78*, 282–285.
18. Yakes, M. K.; Cress, C. D.; Tischler, J. G.; Bracker, A. S. Three-Dimensional Control of Self-Assembled Quantum Dot Configurations. *ACS Nano* **2010**, *4*, 3877–3882.
19. Ohtake, A.; Ozeki, M. *In Situ* Observation of Surface Processes in InAs/GaAs(001) Heteroepitaxy: The Role of As on the Growth Mode. *Appl. Phys. Lett.* **2001**, *78*, 431–433.
20. Heyn, C. Stability of InAs Quantum Dots. *Phys. Rev. B* **2002**, *66*, 075307.
21. Patella, F.; Arciprete, F.; Fanfoni, M.; Balzarotti, A.; Placidi, E. Apparent Critical Thickness versus Temperature for InAs Quantum Dot Growth on GaAs(001). *Appl. Phys. Lett.* **2006**, *88*, 161903.
22. Tok, E.; Neave, J.; Zhang, J.; Joyce, B.; Jones, T. Arsenic Incorporation Kinetics in GaAs(001) Homoepitaxy Revisited. *Surf. Sci.* **1997**, *374*, 397–405.
23. Morgan, C. G.; Kratzer, P.; Scheffler, M. Arsenic Dimer Dynamics during MBE Growth: Theoretical Evidence for a Novel Chemisorption State of As_2 Molecules on GaAs Surfaces. *Phys. Rev. Lett.* **1999**, *82*, 4886–4889.
24. Itoh, M. Atomic-Scale Homoepitaxial Growth Simulations of Reconstructed III-V Surfaces. *Prog. Surf. Sci.* **2001**, *66*, 53–153.
25. Foxon, C.; Joyce, B. Interaction Kinetics of As_4 and Ga on (100) GaAs Surfaces Using a Modulated Molecular Beam Technique. *Surf. Sci.* **1975**, *50*, 434–450.
26. Patella, F.; Nufris, S.; Arciprete, F.; Fanfoni, M.; Placidi, E.; Sgarlata, A.; Balzarotti, A. Tracing the Two- to Three-Dimensional Transition in The InAs/GaAs(001) Heteroepitaxial Growth. *Phys. Rev. B* **2003**, *67*, 205308.
27. Honma, T.; Tsukamoto, S.; Arakawa, Y. *In Situ* Scanning Tunneling Microscope Observation of InAs Wetting Layer Formation on GaAs(001) during Molecular Beam Epitaxy Growth at 500 °C. *Jpn. J. Appl. Phys.* **2006**, *45*, L777–L779.
28. Patella, F.; Arciprete, F.; Fanfoni, M.; Sessi, V.; Balzarotti, A.; Placidi, E. Reflection High Energy Electron Diffraction Observation of Surface Mass Transport at the Two- to Three-Dimensional Growth Transition of InAs On GaAs-(001). *Appl. Phys. Lett.* **2005**, *87*, 252101.
29. Rosini, M.; Kratzer, P.; Magri, R. In Adatom Diffusion On $In_xGa_{(1-x)}As$/GaAs(001): Effects of Strain, Reconstruction and Composition. *J. Phys.: Condens. Matter* **2009**, *21*, 355007.
30. Rosini, M.; Magri, R.; Kratzer, P. Adsorption of Indium on an InAs Wetting Layer Deposited on the GaAs(001) Surface. *Phys. Rev. B* **2008**, *77*, 165323.